Predicting Pseudomorphic Phases in Multilayers: Hexagonal-Closed-Packed Nb in Nb/Zr

G. B. Thompson – The University of Alabama
R. Banerjee – The Ohio State University
H. L. Fraser – The Ohio State University

Citation of published version:

Thompson, G., Banerjee, R., Fraser, H. (2004): Predicting Pseudomorphic Phases in Multilayers: Hexagonal-Closed-Packed Nb in Nb/Zr. *Applied Physics Letters*, 84(7). DOI: https://doi.org/10.1063/1.1647687

Predicting pseudomorphic phases in multilayers: Hexagonal-closed-packed Nb in Nb/Zr

G. B. Thompson[a)]
Department of Metallurgical and Materials Engineering, University of Alabama, Tuscaloosa, Alabama 35487

R. Banerjee and H. L. Fraser
Department of Materials Science and Engineering, The Ohio State University, Columbus, Ohio 43210

(Received 26 August 2003; accepted 17 December 2003)

As the dimensions of materials are reduced to the nanometer scale, changes in phase stability, referred to as pseudomorphism, are being reported. Such changes in phase stability are often serendipitously discovered in multilayered thin films. In this letter, we use a classical thermodynamic treatment to model and predict phase stability in Nb/Zr multilayers. An outcome of this letter is the development of a biphase stability diagram that represents the interrelationship of phase stability to volume fraction and length scale. Using this methodology, an hcp Nb phase stability field was empirically postulated and subsequently confirmed by x-ray and electron diffraction. The successful prediction of this phase, based upon classical thermodynamics quantities, suggests that other types of phase stabilities in other multilayers could be proposed using the biphase diagram. © *2004 American Institute of Physics.* [DOI: 10.1063/1.1647687]

The stabilization of pseudomorphic crystal structures that differ from their bulk equilibrium phases can occur as the size of a material is reduced to the nanoscale regime.[1–8] These changes in crystal structure are often serendipitously discovered. Currently, there appears to be a rather limited understanding of how to model[7,9–11] and predict changes in phase stability. It will be demonstrated in this letter that based on a classical thermodynamic model, it is possible to empirically predict pseudomorphic phases, such as hcp Nb in Nb/Zr thin film multilayers.

Dregia, Banerjee, and Fraser[12] have proposed a classical thermodynamic model to rationalize phase stability in multilayered thin films. In this model, the phase stability in a generic A/B multilayer is considered to be a balance of the volumetric and interfacial components of the free energy. The total free energy of the multilayer can be represented by a unit bilayer of one A layer, one B layer, and two A/B interfaces. The total normalized free energy change of the unit bilayer per unit interfacial area can be represented as the following:[12]

$$\Delta g = [\Delta G_A(1-f_B) + \Delta G_B f_B]\lambda + 2\Delta\gamma, \tag{1}$$

where ΔG_i is the free energy difference per unit volume between the pseudomorphic and bulk phases of i, $\Delta\gamma$ is the corresponding difference in the interfacial energies, λ is the bilayer thickness of layer A plus layer B, and f_i is the volume fraction of i in the multilayer. To maintain the simplicity of Eq. (1), all terms that scale with volume, such as strain, and all terms that scale with area will be included in the respective ΔG_i or $\Delta\gamma$ terms. The additional complexities of such factors can be individually treated within the context of Eq. (1) as needed.[14]

Equation (1) reveals that a multilayered thin film has two degrees of freedom in minimizing the total free energy change. The length scale, λ, and the volume fraction, f_i. A convenient representation of Eq. (1) is the biphase stability diagram.[12] The biphase diagram depicts regions of phase stability as a combination of the two phases, one corresponding to layer A and the other corresponding to layer B, as a function of λ^{-1} and f_i. The biphase diagram provides a quick and simple reference in predicting which combinations of length scale and volume fraction would stabilize a pseudomorphic phase.

Lowe and Geballe[13] reported that for a Zr/Nb multilayer consisting of equally thick Zr and Nb layers ($f_{Nb}=0.5$), the Zr layer exhibits a change in phase stability from hexagonal-closed-packed (hcp) to body-centered-cubic (bcc) when the bilayer thickness is less than 3.1 nm. Coupling this single experimental observation with the classical thermodynamic model,[12] stabilization of pseudomorphic bcc Zr has been predicted and subsequently confirmed[14] for a number of additional Nb/Zr multilayers with $f_{Nb}\neq 0.5$. These experimental data points are plotted in the biphase diagram shown in Fig. 1. The pseudomorphic bcc phase of Zr is a direct consequence of the reduction in Nb/Zr interfacial energy accompanying the transformation from the bulk equilibrium hcp Zr phase to the pseudomorphic bcc Zr phase. The obvious question that arises is if a pseudomorphic bcc form of Zr can be stabilized in relatively Nb-rich Nb/Zr multilayer, is it possible to stabilize a pseudomorphic hcp Nb phase in relatively Zr-rich Nb/Zr multilayer? It should be noted however, that unlike Zr, which undergoes an allotropic transformation from hcp to bcc at 1136 K at 1 atm pressure, no such allotropic transformation from bcc to hcp occurs for elemental Nb.

The classical thermodynamic model provides an empirical framework for predicting the region of phase stability for such a pseudomorphic hcp Nb phase on the Nb/Zr biphase stability diagram. Based on the thermodynamics,[12] the slope, m, of the biphase stability boundary[12] that would separate the hcp Nb/hcp Zr and bcc Nb/hcp Zr biphase fields can be represented as follows:

$$m_{hcp/hcp} = -\Delta G_{Nb}/2\Delta\gamma_{hcp/hcp}, \tag{2}$$

where ΔG_{Nb} is the difference between the volumetric free

a)Electronic mail: gthompson@coe.eng.ua.edu

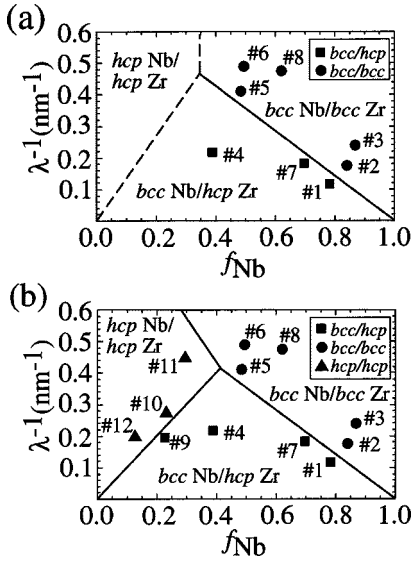

FIG. 1. (a) A predicted biphase stability diagram of Nb/Zr multilayers. The solid line indicates an experimentally determined boundary (Ref. 14) for hcp to bcc transformations for Zr. The dashed boundary, based upon the interfacial energy reduction determined by the solid boundary, represents the predicted stability field for an hcp Nb phase. (b) The complete experimentally determined Nb/Zr biphase stability diagram. As predicted, an hcp Nb phase was confirmed to exist and had reasonably good agreement with the predictions of (a).

energy of hcp Nb and bcc Nb and $\Delta\gamma_{\mathrm{hcp/hcp}}$ is the difference between the interfacial energy of a hcp Nb/hcp Zr interface and a bcc Nb/hcp Zr interface. ΔG_{Nb} being a positive increase in energy would require a specific combination of λ and f_{Nb} such that the negative value of $\Delta\gamma_{\mathrm{hcp/hcp}}$ could dominate Eq. (1) and stabilize the pseudomorphic phase.

The slope of the bcc Nb/bcc Zr–bcc Nb/hcp Zr boundary in Fig. 1(a) can be similarly expressed in the form of Eq. (2) expect the volumetric free energy change is for Zr with its corresponding bcc Nb/bcc Zr interface. From the biphase stability diagram of Fig. 1(a), the experimentally determined slope of the bcc Nb/bcc Zr–bcc Nb/hcp Zr boundary is $-0.72\ \mathrm{nm}^{-1}$. Averaging the atomic volumes for the hcp Zr ($13.5\times10^{-6}\ \mathrm{m}^3/\mathrm{mol}$) and the bcc Zr ($13.4\times10^{-6}\ \mathrm{m}^3/\mathrm{mol}$) phases, the allotropic free energy change[15] was converted into a volumetric free energy change with $\Delta G_{\mathrm{Zr}}=3.7\times10^{8}\ \mathrm{J/m}^3$. Using this slope and the ΔG_{Zr} value, the interfacial free energy difference, $\Delta\gamma_{\mathrm{bcc/bcc}}$, was determined to be approximately $-250\ \mathrm{mJ/m}^2$.

As a first approximation in predicting the hcp Nb/hcp Zr biphase stability field on the Nb/Zr biphase diagram, shown in Fig. 1(a), the value of $\Delta\gamma_{\mathrm{hcp/hcp}}$ was equaled to the experimentally determined value of $\Delta\gamma_{\mathrm{bcc/bcc}}$. Assuming that the atomic volume of hcp Nb is similar to that of bcc Nb, $\Delta G_{\mathrm{Nb}}=9.2\times10^{8}\ \mathrm{J/m}^3$ (Ref. 15) was coupled with $\Delta\gamma_{\mathrm{hcp/hcp}}$ and Eq. (2) in predicting the slope of the hcp Nb/hcp Zr–bcc Nb/hcp Zr boundary. The larger value of ΔG_{Nb} as compared to ΔG_{Zr} suggests that the hcp Nb/hcp Zr stability region would be rather limited in extent as compared to the bcc Nb/bcc Zr phase field. The predicted bcc Nb/hcp Zr–hcp Nb/hcp Zr biphase boundary has been plotted as a dashed line in Fig. 1(a). In order to experimentally test the existence of the predicted region of hcp Nb phase stability, a set of relatively Zr-rich Nb/Zr multilayers, corresponding to the points marked 9, 10, 11, and 12 on Fig. 1(b), have been sputtered deposited.

The multilayers were grown in an ultrahigh vacuum stainless steel chamber with a base pressure of $\sim4\times10^{-9}$ Torr. Ultrahigh-purity Ar, at a working pressure of 3.1 mTorr, was used as the sputtering gas. The substrates were $\langle111\rangle$ Si wafers that have a 200-nm-thick amorphous oxide layer on the surface preventing any epitaxial orientation relationship to develop between film and substrate. Forty bilayers were deposited for each specimen. The multilayers were characterized in the as-deposited state (on the substrate) by reflection x-ray diffraction (RXRD) in the Bragg–Brentano geometry and transmission x-ray diffraction (TXRD). These XRD techniques require no sample preparation thereby eliminating the possibility for specimen preparation artifacts. RXRD was conducted in a Scintag XDS 2000 X-Ray Diffractometer using Cu $K\alpha$ radiation (0.154 nm). The films grew with a preferred growth texture that corresponded to their closet packed planes, e.g., {011} bcc and/or {0002} hcp. TXRD was performed at the Advanced Photon Source UNI-CAT Beamline 33BM facility at Argonne National Laboratory. The synchrotron energy was fixed at 15.05 keV (0.0821 nm) and penetrated through both the Si substrate and the mutlilayered film. Additionally, the multilayers were characterized in the plan-view geometry using a Philips CM 200 transmission electron microscope (TEM). TEM bright-field images in the plan-view geometry indicated that the films were polycrystalline with grain diameters of 15–50 nm. Cross-section TEM foils were prepared in a FEI DB-235 Focused Ion Beam instrument. The cross-section TEM bright-field columnar grain diameters matched well with the plan-view polycrystalline diameters. The chemical composition of the multilayers was determined using energy dispersive spectroscopy performed in a Phillips/FEI XL30 FEG Scanning Electron Microscope. The bilayer spacing was calculated from the separation in satellite diffraction peaks that arise from the chemical modulation of the multilayer's stacking sequence taken in the RXRD geometry.

The TXRD pattern of the Nb/Zr No. 10 multilayer is shown in Fig. 2(a). The hexagonal $\{10\bar{1}0\}$ reflection is present but no bcc Nb {110} reflection is observed. This is apparent by comparing this pattern with the TXRD pattern from a bcc Nb/hcp Zr multilayer, shown in Fig. 2(b), which corresponds to the multilayer marked No. 1 in Fig. 1(b). The location of the {110} Nb reflection, with a full-width at half-maximum peak position at 20.3° 2θ, is clearly seen in Fig. 2(b). The absence of this peak for multilayer No. 10 indicates that the Nb layers have undergone a change in phase stability. In the TXRD pattern shown in Fig. 2(a), the $\{10\bar{1}0\}$ hcp and $\{10\bar{1}1\}$ hcp peaks are visible. From the asymmetry (or split) in these peaks, as shown by the inset diffraction patterns of Fig. 2(a), it is apparent that there is an overlap of two distinct reflections corresponding to two sets of hcp lattice parameters. Pseudo-Voight deconvolution of the asymmetric $\{10\bar{1}0\}$ peak was used to calculate the a-lattice parameters for the two hcp phases. Subsequently, using these a-lattice parameters, the c parameter for each of the hcp phases was calculated from the split in the $\{10\bar{1}1\}$ TXRD inset figure of Fig. 2(a). The TXRD c-lattice parameters were in good agreement with the c parameters determined by the Pseudo–

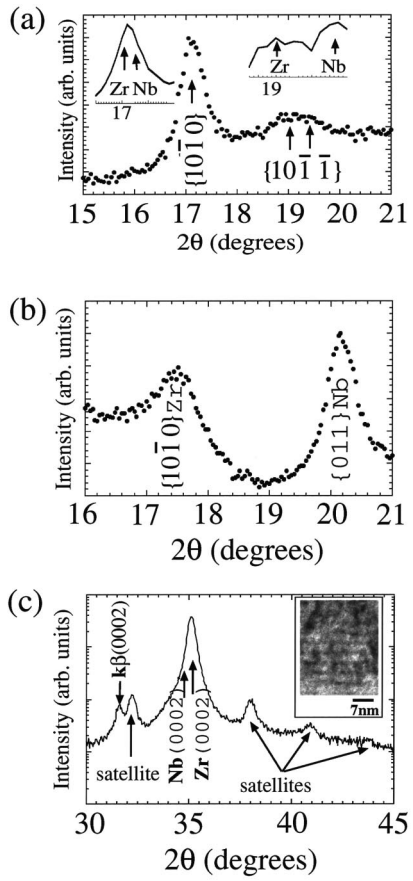

FIG. 2. X-ray diffraction of hcp Nb/hcp Zr. (a) TXRD pattern, with $\{10\bar{1}0\}$ and $\{10\bar{1}1\}$ reflections present, for the hcp Nb/hcp Zr multilayer (No. 10). The insets are high resolution scans of the hcp reflections. (b) TXRD pattern for the bcc Nb/hcp Zr multilayer (No. 1). The peaks' positions for the hcp Zr $\{10\bar{1}0\}$ and the bcc Nb $\{110\}$ reflections are present for comparison to (a). (c) RXRD pattern of the hcp Nb/hcp Zr multilayer (No. 10). The $\{0002\}$ peak is slightly asymmetric. Deconvolution confirmed that the *c*-lattice parameters, calculated from the $\{10\bar{1}1\}$ reflections of (a), matched to this peak. Satellite reflections from the periodic layering of the multilayer were used to accurately determine the bilayer spacing of the multilayer. The inset TEM bright-field many-beam cross-section image confirms the morphologically sharp interfaces of the layered structure.

Voight deconvolution of the $\{0002\}$ intensity in the RXRD pattern from the same multilayer shown in Fig. 2(c). The lack of a significant split in the $\{0002\}$ peak in Fig. 2(c) for the two-hcp phases is due to the substantially lower volume fraction of one phase (Nb) as compared to the other (Zr). Even so, a point of inflection is clearly visible in the slightly asymmetric $\{0002\}$ peak. The respective lattice parameters for each hcp phase, as determined by XRD, in the as-deposited state are listed as the following:

$$a_1 = 3.15\ \text{Å}; \quad c_1 = 5.12\ \text{Å}\ \text{(phase 1)},$$

$$a_2 = 3.21\ \text{Å}; \quad c_2 = 5.10\ \text{Å}\ \text{(phase 2)}.$$

In addition to the primary $\{0002\}$ peak, satellite peaks are visible in the RXRD pattern shown in Fig. 2(c). The presence and number of distinct satellite reflections in the RXRD pattern indicates that the film has maintained a layered structure. This was confirmed by a cross-section bright-field TEM micrograph, placed as an inset in Fig. 2(c), of this multilayer. The XRD identified phases were also corroborated by plan-view TEM diffraction.[16]

The experimentally determined biphase boundary between the hcp Nb/hcp Zr and bcc Nb/hcp Zr biphase fields has been marked by a solid line in Fig. 1(b). Using the experimentally determined slope of the hcp Nb phase boundary, the value of $\Delta\gamma_{\text{hcp/hcp}}$ has been determined. The experimentally determined hcp Nb lattice parameters were used to refine the atomic volume average used in the calculation of the volumetric free energy difference (ΔG_{Nb}). The refined ΔG_{Nb} value is $7.5\times10^8\ \text{J/m}^3$. Using this value and the experimentally determined slope, $0.86\ \text{nm}^{-1}$, $\Delta\gamma_{\text{hcp/hcp}} \approx -480\ \text{mJ/m}^2$.

In summary, a classical thermodynamic treatment of phase stability in multilayered materials allowed for the prediction of a pseudomorphic hcp Nb phase in Nb/Zr multilayers. The formation of this phase has been systematically predicted and experimentally confirmed rather than being serendipitously discovered. The hcp Nb phase adopts its own lattice parameters that are different from those of hcp Zr. Based on these observations, a complete Nb/Zr phase stability diagram has been constructed which can be used as a tool to predict the combinations of volume fractions and length scales that can stabilize pseudomorphic phases in this system.

The authors thank the *Center for the Accelerated Maturation of Materials* (CAMM) at The Ohio State University for funding this research. The UNICAT facility at the Advanced Photon Source (APS) is supported by the Univ. of Illinois at Urbana-Champaign, Materials Research Laboratory (U.S. DOE, the State of Illinois-IBHE-HECA, and the NSF), the Oak Ridge National Laboratory (U.S. DOE under contract with UT-Battelle LLC), the National Institute of Standards and Technology (U.S. Department of Commerce) and UOP LLC. The APS is supported by the U.S. DOE, Basic Energy Sciences, Office of Science under Contract No. W-31-109-ENG-38.

[1] W. A. Jesser and J. W. Matthews, Philos. Mag. **15**, 1097 (1967).
[2] H. Wormeester, E. Hüger, and E. Bauer, Phys. Rev. Lett. **77**, 1540 (1996).
[3] R. Banerjee, S. A. Dregia, and H. L. Fraser, Acta Mater. **47**, 4225 (1999).
[4] W. Vavra, D. Barlett, S. Egaloz, C. Uher, and R. Clarke, Phys. Rev. B **47**, 5500 (1993).
[5] N. Metoki, W. Donner, and H. Zabel, Phys. Rev. B **49**, 17351 (1994).
[6] G. A. Prinz, Phys. Rev. Lett. **54**, 1051 (1985).
[7] A. A. Mbaye, D. M. Wood, and A. Zunger, Phys. Rev. B **37**, 3008 (1998).
[8] A. Madan, I. W. Kim, S. C. Cheng, P. Yashar, V. P. Dravid, and S. A. Barnett, Phys. Rev. Lett. **78**, 1743 (1997).
[9] E. S. Machlin, *An Introduction to Aspects of Thermodynamic and Kinetics Relevant to Materials Science* (Giro, Croton-on-Hudson, NY, 1991), p. 131.
[10] R. Buinsma and A. M. Zangwill, J. Phys.: Condens. Matter **47**, 2055 (1986).
[11] A. C. Redfield and A. M. Zangwill, Phys. Rev. B **34**, 1378 (1986).
[12] S. A. Dregia, R. Banerjee, and H. L. Fraser, Scr. Mater. **29**, 217 (1998).
[13] W. P. Lowe and T. H. Geballe, Phys. Rev. B **29**, 4961 (1984).
[14] G. B. Thompson, R. Banerjee, S. A. Dregia, and H. L. Fraser, Acta Mater. **51**, 5285 (2003).
[15] A. F. Guillermet, Z. Metallkunde **82**, 478 (1991).
[16] G. B. Thompson, *Predicting Polymorphic Phase Stability in Multilayered Thin Films*, PhD dissertation, The Ohio State University, Columbus, OH, 2003.